Temporal and Spacial Evolution of Bursts in Creep Rupture

Zsuzsa Danku and Ferenc Kun*

Department of Theoretical Physics, University of Debrecen, P.O. Box 5, H-4010 Debrecen, Hungary

(Received 14 February 2013; published 21 August 2013)

We investigate the temporal and spacial evolution of single bursts and their statistics emerging in heterogeneous materials under a constant external load. Based on a fiber bundle model we demonstrate that when the load redistribution is localized along a propagating crack front, the average temporal shape of pulses has a right-handed asymmetry; however, for long range interaction a symmetric shape with parabolic functional form is obtained. The pulse shape and spatial evolution of bursts proved to be correlated, which can be exploited in materials' testing. The probability distribution of the size and duration of bursts have power law behavior with a crossover to higher exponents as the load is lowered. The crossover emerges due to the competition of the slow and fast modes of local breaking being dominant at low and high loads, respectively.

DOI: 10.1103/PhysRevLett.111.084302 PACS numbers: 46.50.+a, 05.90.+m, 62.20.mm, 89.75.Da

Crackling noise is a generic feature of a wide variety of slowly driven dynamic systems such as ferromagnetic materials, plastically deforming crystals, superconductors, fracture processes of heterogeneous materials, and earthquakes [1–6]. Analyzing the time series of crackling events, it was shown that crackling phenomena exhibit a high degree of universality [1,4]. The size and duration of events and, furthermore, the waiting times in between are characterized by power law distributions with the same exponents in systems of different microscopic dynamics. Recently, it has been demonstrated for Barkhausen noise that there are unique features of crackling which go beyond universality; i.e., the average temporal shape of single burst pulses proved to provide direct information about the nature of correlations in the microscopic dynamics [2,3,7–9]. For systems where the impulsive relaxation mechanism competes with slow ones, a novel phase of crackling has been discovered very recently [5]. When the rate of external driving becomes comparable to the time scale of slow relaxation, large bursts emerge in a quasiperiodic manner, which is accompanied by a crossover in the statistics of burst sizes and durations.

We present a theoretical investigation of crackling noise emerging during the creep rupture of heterogeneous materials focusing on single burst dynamics in the presence of two competing failure mechanisms. Creep rupture has a high technological importance for the safety of construction components, and it is at the core of natural catastrophes such as landslides as well as stone and snow avalanches [10]. Crackling during creep is the consequence of the intermittent nucleation and propagation of cracks which generate acoustic bursts. Despite the intensive research on rupture phenomena [4,6,10–17], the temporal and spatial evolution of single bursts, the effect of the competition of failure mechanisms with different time scales, and their relevance for applications still remained an open fundamental problem.

To investigate the creep rupture of heterogeneous materials we use a generic fiber bundle model (FBM) introduced recently [18–20]: the sample is discretized as a bundle of fibers on a square lattice of side length L. Fibers have a brittle response with identical Young modulus E. The bundle is subject to a constant external load σ_0 below the fracture strength σ_c of the system parallel to the fibers. Fibers break due to two physical mechanisms: immediate breaking occurs when the local load σ_i on fibers exceeds their fracture strength σ_i^{th}. Time dependence is introduced such that those fibers, which remained intact, undergo an aging process accumulating damage $c_i(t)$. The damage mechanism represents the environmentally induced slowly developing aging of materials, e.g., thermally activated degradation [18–20]. The rate of damage accumulation Δc_i is assumed to have a power law dependence on the local load $\Delta c_i = a\sigma_i^{\gamma}\Delta t$, where $a = 1$ is a constant and the exponent γ controls the time scale of the aging process with $0 \leq \gamma < +\infty$. Fibers can tolerate only a finite amount of damage and break when $c_i(t)$ exceeds the local damage threshold c_i^{th}. Each breaking event is followed by a redistribution of load over the remaining intact fibers. To capture the effect of the inhomogeneous stress field around cracks, we assume localized load sharing (LLS); i.e., the load of broken fibers is equally redistributed over their intact nearest neighbors [20]. The structural disorder of the material is represented by the randomness of breaking thresholds σ_i^{th}, c_i^{th}, $i = 1, \ldots, N = L^2$. We assume that both thresholds are uniformly distributed in an interval $[1-\delta, 1+\delta]$, where $\delta = 1$ (high disorder) for σ^{th}. To promote the effect of stress concentrations, lower disorder $\delta = 0.3$ is considered for damage c^{th}, while the exponent γ of the damage law is set to a high value $\gamma = 5$ [20]. In the following, simulation results will be presented for the lattice size $L = 401$, larger system sizes up to $L = 1201$ are considered for finite size scaling analysis.

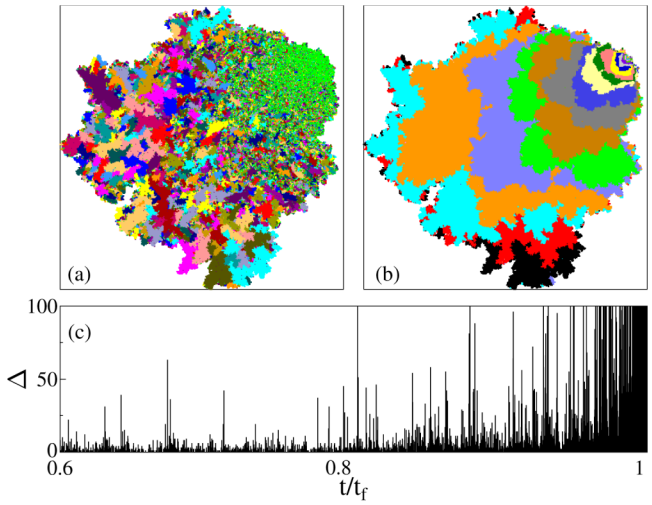

FIG. 1 (color online). (a) Bursting activity during the creep rupture of a fiber bundle of size $L = 401$. Slowly damaging fibers (green-shade of gray in the upper right corner) trigger bursts of immediate breaking (random colors-shades of gray-different from green). The crack started in the upper right corner of the figure. (b) Advancement of the front of the same crack obtained such that fibers broken in a time interval have the same color. (c) Time series of bursts of (a) as a stochastic point process.

Figure 1(a) presents an example of the time evolution of a crack in our FBM under the load $\sigma_0/\sigma_c = 0.01$. The separation of time scales of the slow damage process and of immediate breaking leads to a highly complex time evolution in agreement with experiments [18,19]: after the crack nucleated, fibers mostly break due to slow damaging and generate an advancing crack front where the stress of broken fibers is concentrated. Beyond a certain crack size the subsequent load increments become sufficient to trigger bursts of immediate breakings locally accelerating the front. As a consequence, the time evolution of creep rupture occurs as a series of bursts separated by silent periods of slow damaging. The size of bursts Δ is defined as the number of fibers breaking in a correlated trail. For clarity, in Fig. 1(b) the crack front is presented at several times, while Fig. 1(c) shows the time series of bursts, i.e., the burst size Δ as a function of time t normalized with the lifetime t_f of the system [12–14,19,20]. See Supplemental Material [21] for an animation of the bursty crack growth.

Single bursts typically start with the immediate breaking of a few fibers. Because of load redistribution, additional breakings are triggered so that bursts gradually evolve through subavalanches and stop when all the intact fibers along the burst boundary can sustain the local load. This avalanche dynamics is controlled by the range of interaction so that similar evolution would arise under quasistatically increasing external load, as well [18–20,22]. Figure 2 presents for a burst of size $\Delta = 3485$ that the outbreak starts from a small localized spot which then gradually expands to a broad region followed by the subsequent reduction of the breaking activity. The temporal profile

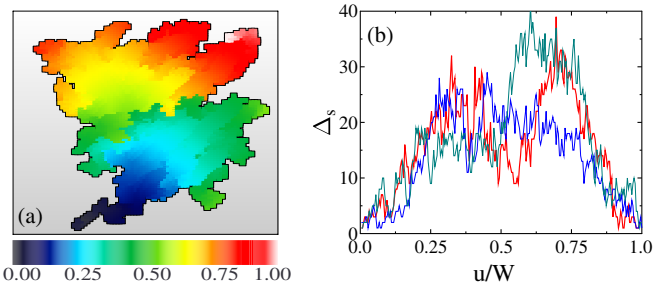

FIG. 2 (color online). (a) Temporal and spatial evolution of a single burst of size $\Delta = 3485$. The color code represents the normalized time $0 \le u/W \le 1$. The burst starts from a small spot of broken fibers (blue-black) at the bottom left corner, then it gradually expands (green, yellow, red-lighter shades of gray) and finally stops again in a small spot (white) at the top right corner. (b) The size of subbursts Δ_s as a function of u/W for a fixed duration $W = 253$. The red curve corresponds to the burst of (a).

of bursts can be characterized by recording the size Δ_s of subavalanches as a function of the internal time step u over the duration W of the burst, where $1 \le u \le W$ holds. Comparing $\Delta_s(u)$ curves of bursts of the same duration $W = 253$ in Fig. 2(b) the stochastic nature of avalanche dynamics is apparent.

The average pulse shape $\langle \Delta_s(u, W) \rangle$ of bursts is presented in Fig. 3(a) as a function of time u varying the pulse duration W. The $\langle \Delta_s(u, W) \rangle$ curves have a right-handed asymmetry; i.e., they can be described by a nearly parabolic shape where the maximum of the inverted parabola is shifted from the middle $(W/2)$ to higher values. Figure 3(b) demonstrates that rescaling $\langle \Delta_s(u, W) \rangle$ with an appropriate power α of the duration W, the pulse shapes of different W can be collapsed on a master curve as a function of the normalized time $x = u/W$. The good quality data collapse implies the scaling form

$$\langle \Delta_s(u, W) \rangle = W^{\alpha} f(u/W), \tag{1}$$

where both the scaling function $f(x)$ and the scaling exponent α encode information about the jerky crack propagation. The right-handed asymmetry of the scaling function $f(x)$ shows that bursts start slowly, then gradually accelerate, and finally stop suddenly as the front gets pinned. The average pulse shape can be described by the function $f(x) = Ax(1 - x)^{\beta}$, where A determines the initial acceleration and the exponent $\beta < 1$ describes the observed right-handed asymmetry. In Fig. 3(b) collapse was achieved with $\alpha = 0.7$, while the fit of the scaling function was obtained with $A = 4.65$ and $\beta = 0.65$.

In order to understand the role of the range of load sharing in shaping temporal pulses, we analyzed the mean field limit of our FBM [18–20]. In this case the load of broken fibers is equally shared by all the remaining intact ones so that no stress concentration, and hence, no spatial correlation can arise in the bundle [22]. Figure 3(b) presents the scaling function $f(x)$ of the mean field

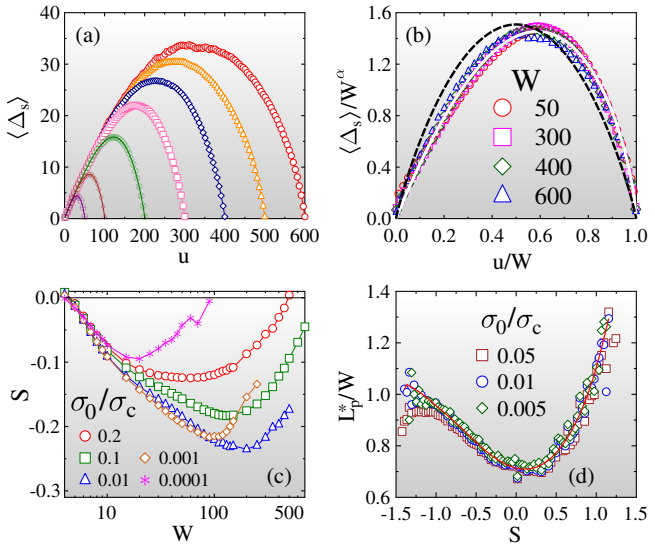

FIG. 3 (color online). (a) Average pulse shapes for durations $W = 50, 100, 200, 300, 400, 500, 600$ for LLS FBMs obtained at the load $\sigma_0/\sigma_c = 0.01$. (b) Scaling collapse of average pulse shapes of different duration for LLS. The white continuous line represents the fit with the scaling function $f(x)$. The dashed black line presents the scaling function of the mean field limit of FBM for comparison. (c) Skewness S of pulse shapes as a function of the duration W at different loads. (d) The number of perimeter sites of bursts touching the crack front L_p^* divided by the duration W as a function of the corresponding skewness of bursts.

simulations of a bundle of $N = 10^7$ fibers, where the symmetric parabolic shape is evidenced with the scaling exponent $\alpha = 1$, similarly to mean field avalanches of slip events in plastically deforming solids, and of particle rearrangements in sheared granular matter [2–4,7].

To quantify the degree of asymmetry of pulse shapes we calculated the skewness S as a function of W, where S is defined as the ratio of the third cumulant and the $3/2$ power of the second cumulant of the pulse [2]. In Fig. 3(c) the skewness S of pulse shapes is negative in agreement with the observed right-handed asymmetry; however, the value of S has a strong dependence on the pulse duration W: short pulses are flat and symmetric; hence, $S \approx 0$ follows in this range. Bursts of high duration tend again to be symmetric, since as they evolve the structural disorder of the material becomes dominating, which favors symmetric pulse shapes [2–4,7]. The most remarkable feature is that at each load a characteristic time scale $W_{\max}$ emerges where the degree of asymmetry $|S|$ has a maximum. Both the characteristic duration $W_{\max}$ and strength of asymmetry $|S|_{\max}$ of pulses have a strong dependence on the external load σ_0/σ_c, and they reach a maximum nearly at the same load $\sigma_0/\sigma_c \approx 0.01$.

After starting from a localized spot, an avalanche has more chance to advance if subbursts involve overloaded fibers at the front, as well, instead of just propagating forward ahead of the crack front [see Figs. 1(a) and 1(b)]. Consequently, the temporal profile and the geometry of avalanches with respect to the local position along the crack front get correlated. To quantify this correlation we measured the number of those perimeter sites L_p^* of bursts which are located at the crack front. In Fig. 3(d) the value of the ratio L_p^*/W is plotted as a function of the skewness S of the corresponding pulse. For symmetric pulses ($S \approx 0$) the ratio L_p^*/W has a low value which shows that these bursts were mainly moving forward where structural disorder dominates. However, for asymmetric pulses L_p^*/W increases so that these avalanches involve a large fraction of overloaded fibers at the crack front which accelerates spreading. Our result has the important consequence that by measuring pulse shapes one can infer the spatial propagation of bursts.

Equation (1) implies that the average burst size $\langle\Delta\rangle$ must scale with the duration as $\langle\Delta\rangle \sim W^{1+\alpha}$. To verify the scaling structure we determined the function $\langle\Delta\rangle$ (W) numerically by directly averaging the size of bursts Δ at fixed durations W. It can be observed in Fig. 4(a) that the simulation results agree very well with the analytic prediction; however, the asymptotic value of the power law exponent depends on the external load: at low loads the average burst size proved to be proportional to the duration $\langle\Delta\rangle \sim W$ with $\alpha = 0$. Consequently, in this load range the pulse shape is not parabolic, but instead it has a flat, symmetric functional form [15–17] in agreement with the skewness value $S \approx 0$ [see also Fig. 3(c)]. During the creep process the external load controls the relative importance of slow damaging and immediate breaking. At high load $\sigma_0 \to \sigma_c$ already a few damage breakings are sufficient to trigger extended bursts so that their size increases faster with the duration characterized by a higher exponent $\langle\Delta\rangle \sim W^{1.7}$ with $\alpha = 0.7$ [see Fig. 4(a)]. This crossover has also important consequences for the statistics of the size and duration of bursts. In Figs. 5(a) and 5(b) the probability distribution of the burst size $p(\Delta)$ and duration $p(W)$ have power law functional form at all load values followed by a cutoff

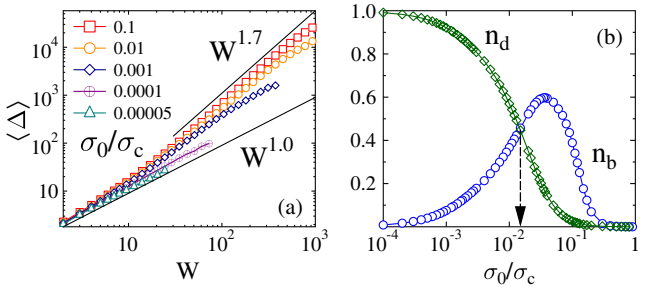

FIG. 4 (color online). (a) Average size of bursts $\langle\Delta\rangle$ as a function of the duration W for several load values σ_0. (b) The fraction of fibers breaking due to damage n_d and to avalanches n_b as function of σ_0.

$$p(\Delta) = \Delta^{-\tau} g(\Delta/\Delta_0), \qquad p(W) = W^{-z} h(W/W_0), \qquad (2)$$

where the functions $g(x)$ and $h(x)$ can be well approximated by exponentials. A very important feature of the results is that not only do the cutoffs Δ_0 and W_0 depend on the external load σ_0, but also the distributions exhibit a crossover between two regimes of different exponents. The crossover point $\sigma_0^*/\sigma_c = 0.025(4)$ falls close to the load where bursts reach the highest asymmetry [compare to Fig. 3(c)]. It is important to note that the crossover emerges due to the competition of the slow and fast breaking modes of fibers as the external load is varied, in a close analogy to the mechanism which leads to the self-organized avalanche oscillator in crystal plasticity [5]. At high loads $\sigma_0 > \sigma_0^*$ large avalanches are triggered with longer durations; however, when approaching the critical load σ_c it gets more likely that once an avalanche started it cannot stop and leads to catastrophic failure. Consequently, the power law exponents τ and z have relatively low values $\tau = 1.75$ and $z = 1.82$, and the cutoffs Δ_0 and W_0 decrease with increasing load σ_0 [see Figs. 5(a) and 5(b)]. On the contrary, low load $\sigma_0 < \sigma_0^*$ favors the damage breaking; i.e., long damage sequences are needed to trigger bursts which have rather limited sizes. Hence, this regime is characterized by higher exponents $\tau = 2.4$ and $z = 2.55$ of the distributions $P(\Delta)$ and $P(W)$ and the cutoffs Δ_0 and W_0 increase when approaching the crossover load from below. To quantify the relative importance of the slow and fast failure modes we determined the fraction of fibers breaking due to damage n_d and in avalanches n_b as a function of load. It can be seen in Fig. 4(b) that the fraction n_d of damage breakings monotonically decreases with σ_0, while n_b first increases and has a maximum at $\sigma_0/\sigma_c = 0.045(6)$. Note that the two fractions become equal $n_d = n_b$ at the load $\sigma_0/\sigma_c = 0.018(5)$, which falls very close to the crossover point supporting the above arguments. To analyze the finite size dependence of the distributions $p(\Delta)$ and $p(W)$ we carried out simulations at fixed loads for several lattice sizes $L = 401, 601, 801, 1001, 1201$. As representative examples, Fig. 5(c) presents for two load values $\sigma_0/\sigma_c = 0.1$ and 0.001 that the cutoff burst size of $p(\Delta, L)$ increases with the system size L. Rescaling the two axis with appropriate powers of L a high quality data collapse is obtained in Fig. 5(d) which implies the scaling structure $p(\Delta, L) = \Delta^{-\tau}\phi(\Delta/L^{\xi})$. The cutoff exponent ξ has the values 2.4, 1.3 ($\sigma_0 < \sigma^*$) and 1.6, 1.0 ($\sigma_0 > \sigma^*$), for the distribution of burst sizes and durations, respectively. The analysis demonstrates the robustness of the critical exponents τ and z of the system.

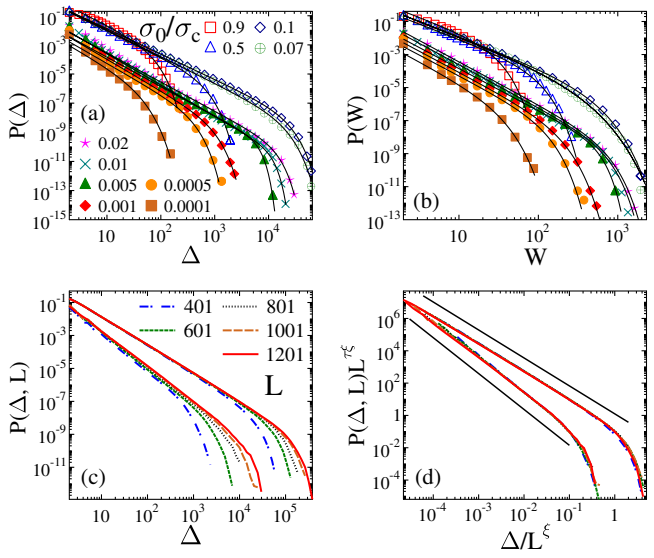

FIG. 5 (color online). Probability distribution of burst size $p(\Delta)$ (a) and duration $p(W)$ (b) varying the external load σ_0. The lines are fits with Eqs. (2). (c) Burst size distributions for different system sizes L obtained at two load values $\sigma_0/\sigma_c = 0.1$ and 0.001 for the upper and lower groups of curves, respectively. (d) High quality collapse of the distributions of (c) obtained by rescaling with L using the scaling exponents $\xi = 1.6$, $\tau = 1.75$ and $\xi = 2.4$, $\tau = 2.4$ for the lower and upper curves, respectively. The straight lines represent power laws of slope τ. In (a) and (b) the vertical axis, while in (d) both axis are arbitrarily rescaled to better see the data.

In conclusion, investigating the dynamics of single bursts in FBMs we revealed a rich spectrum of novel aspects of rupture processes. The average shape of burst pulses proved to be sensitive to the range of load redistribution. Since the evolution of bursts is controlled by the overloads at the avalanche frontier, we revealed that from the temporal pulse shape one can infer the spatial advancement of bursts. The statistics of burst sizes and durations is characterized by power law distributions; however, the competition of the failure modes with widely separated time scales leads to the emergence of a crossover between two regimes of different exponents: approaching the critical load large bursts are triggered implying low exponents for the distributions, while below a characteristic load slow damaging dominates giving rise to higher exponents. A very interesting future extension of our study is to perform tests where σ_0 is increased at a constant rate r. The current calculations are at the limiting case $r = 0$. Under such conditions avalanche precursors are expected in the time series as r increases, namely, quasiperiodic large avalanches, before rupture, as predicted and observed in the modeling and experimental approach of Ref. [5] in the context of crystal plasticity and consistently observed in granular experiments of avalanches in jammed granular matter at an incline [23]. The quasiperiods of events emerge due to the dynamic competition between the two time scales of the external driving and the intrinsic aging [5].

We are thankful for Projects No. TAMOP-4.2.2.A-11/1/KONV-2012-0036, No. TAMOP-4.2.2/B-10/1-2010-0024, No. TAMOP 4.2.4.A/2-11-1-2012-0001, No. OTKA K84157, and No. ERANET_HU_09-1-2011-0002.

*ferenc.kun@science.unideb.hu

[1] J. P. Sethna, K. A. Dahmen, and C. R. Meyers, Nature (London) **410**, 242 (2001).
[2] S. Papanikolaou, F. Bohn, R. L. Sommer, G. Durin, S. Zapperi, and J. P. Sethna, Nat. Phys. **7**, 316 (2011).
[3] S. Zapperi, C. Castellano, F. Colaiori, and G. Durin, Nat. Phys. **1**, 46 (2005).
[4] K. A. Dahmen, Y. Ben-Zion, and J. T. Uhl, Nat. Phys. **7**, 554 (2011).
[5] S. Papanikolaou, D. M. Dimiduk, W. Choi, J. P. Sethna, M. D. Uchic, C. F. Woodward, and S. Zapperi, Nature (London) **490**, 517 (2012).
[6] M. J. Alava, P. K. V. V. Nukala, and S. Zapperi, Adv. Phys. **55**, 349 (2006).
[7] A. Baldassarri, F. Colaiori, and C. Castellano, Phys. Rev. Lett. **90**, 060601 (2003).
[8] A. P. Mehta, A. C. Mills, K. A. Dahmen, and J. P. Sethna, Phys. Rev. E **65**, 046139 (2002).
[9] L. Laurson and M. J. Alava, Phys. Rev. E **74**, 066106 (2006).
[10] G. Niccolini, A. Carpinteri, G. Lacidogna, and A. Manuello, Phys. Rev. Lett. **106**, 108503 (2011).
[11] C. Maes, A. Van Moffaert, H. Frederix, and H. Strauven, Phys. Rev. B **57**, 4987 (1998).
[12] H. Nechad, A. Helmstetter, R. El Guerjouma, and D. Sornette, Phys. Rev. Lett. **94**, 045501 (2005).
[13] J. Rosti, X. Illa, J. Koivisto, and M. J Alava, J. Phys. D **42**, 214013 (2009).
[14] S. Deschanel, L. Vanel, N. Godin, G. Vigier, and S. Ciliberto, J. Stat. Mech. (2009) P01018.
[15] K. J. Maloy, S. Santucci, J. Schmittbuhl, and R. Toussaint, Phys. Rev. Lett. **96**, 045501 (2006).
[16] D. Bonamy, S. Santucci, and L. Ponson, Phys. Rev. Lett. **101**, 045501 (2008).
[17] K. T. Tallakstad, R. Toussaint, S. Santucci, J. Schmittbuhl, and K. J. Maloy, Phys. Rev. E **83**, 046108 (2011).
[18] F. Kun, M. H. Costa, R. N. C. Filho, J. S. Andrade, J. B. Soares, S. Zapperi, and H. J. Herrmann, J. Stat. Mech. (2007) P02003.
[19] F. Kun, H. A. Carmona, J. S. Andrade, Jr., and H. J. Herrmann, Phys. Rev. Lett. **100**, 094301 (2008).
[20] Z. Halász, Zs. Danku, and F. Kun, Phys. Rev. E **85**, 016116 (2012).
[21] See Supplemental Material at http://link.aps.org/supplemental/10.1103/PhysRevLett.111.084302 for animation of the propagation of a single crack during the creep process. Damaging fibers (green) trigger bursts of immediate breakings (randomly selected colors different from green).
[22] S. Pradhan, A. Hansen, and P. C. Hemmer, Phys. Rev. Lett. **95**, 125501 (2005); S. Pradhan, A. Hansen, and B. K. Chakrabarti, Rev. Mod. Phys. **82**, 499 (2010).
[23] S. Kiesgen de Richter, V. Y. Zaitsev, P. Richard, R. Delannay, G. Le Caër, and V. Tournat, J. Stat. Mech. (2010) P11023.